Focused Ion Beam Micro- and Nanoengineering

Richard M. Langford, Philipp M. Nellen, Jacques Gierak, and Yongqi Fu

Abstract

This article discusses applications of focused ion beam micro- and nanofabrication. Emphasis is placed on illustrating the versatility of focused ion beam and dual-platform systems and how they complement conventional processing techniques. The article is divided into four parts: maskless milling, ion beam lithography, ion implantation, and techniques such as *in situ* micromanipulation.

Introduction

Focused ion beam (FIB) and dual-platform systems (i.e., systems with both ion and electron beam columns) have been used extensively for microfabrication and nanofabrication during the past 10–15 years, for example, for circuit modifications[1] and read–write head trimming.[2] The tools can sputter and implant lines as narrow as 10 nm and deposit metals and insulators in lines as narrow as 30 nm in user-defined patterns. In addition, as the FIB is scanned, signals such as the generated secondary electrons (SE) can be collected for imaging. It is the combination of these capabilities that is at the heart of the instrument's power and versatility for micro- and nanofabrication; a device or sample may be imaged and the FIB sputtering or metal/insulator deposition can then be made to within 50 nm of a feature or area of interest.

Over the last five years, there has been a marked increase in the diversity and complexity of the applications for these systems. This has been driven partly by the nanotechnology explosion but is mainly because the increased number of systems installed in academia and industry has provided greater access.

This article reviews FIB micro- and nanofabrication applications. Only selected examples are given, because the use of these fabrication systems has become very diverse. Emphasis is placed on illustrating their versatility, how they complement conventional processing, and applications that are pushing the boundaries of nanocharacterization and fabrication.

These tools (subsequently referred to as FIB systems) complement conventional fabrication equipment, and typically their use falls into one of two categories. The first category is the fabrication or modification of structures and devices that are difficult to prepare using conventional processes because of material or geometry constraints. For example, Lacour et al.[3] FIB-patterned periodic structures into a $LiNbO_3$ film, which is difficult to do using dry etching. The second category is the rapid prototyping or modification of structures and devices, which can be done in fewer, quicker, and simpler processing steps when using an FIB system than is possible using conventional processing. For example, if nanowires and carbon nanotubes[4,5] are dispersed to within 20 μm of pre-patterned electrodes and contact pads, *in situ* ion and electron beam–assisted deposition can be used to contact them to the pre-patterned electrodes in less than 30 minutes. In contrast, using electron beam lithography and metal lift-off can take up to two days. The most time-consuming steps involve measuring the position of the nanowires relative to alignment crosses and modifying the computer-aided design drawings.

This article is divided into four sections. The first section discusses FIB micro- and nanomilling and covers aspects such as pattern densities and milling three-dimensional (3D) shapes. The second section covers FIB lithography, that is, Ga implantation or milling followed by a pattern transfer or growth step. The third section discusses FIB implantation for patterning and device fabrication. The fourth section highlights other fabrication techniques such as *in situ* micromanipulation. The article concludes with a discussion of possible future developments for enhancing the nanofabrication capabilities of FIB systems.

FIB Micro- and Nanomilling

FIB milling, whether for sample preparation for electron microscopy or direct maskless patterning, is the most commonly used application of the systems and has been used to prepare a range of devices including lenses on the ends of fibers,[6] pseudo spin valves,[7] pillar microcavities,[8] and stacked Josephson junctions.[9]

The smallest ion beam spot size is approximately 5–10 nm, which enables correspondingly small features to be patterned. The shape of an FIB cut is dependent on many factors, such as its geometry, milled depth, ion beam profile, and the redeposition of sputtered material. (Other factors, such as self-focusing, are discussed in the section "Micromachining 3D Structures with Complicated Shapes"). The combination of ion beam profile effects and sputter yield changes with the FIB angle of incidence causes rounding of the top edges of an FIB cut and the sidewalls to be inclined a few degrees from the perpendicular (the exact angles depend on the ion beam profile and milled depth). Redeposition may also cause the sidewalls to incline.

As the milling depth increases, the probability of the sputtered material redepositing onto the sidewalls increases. If a line or hole is milled 10 to 15 times deeper than its width, redeposition results in V-shaped cross sections. The aspect ratio (depth to width) can be improved by using gas-enhanced etching (see the article by MoberlyChan et al. in this issue). Because the shape of a cut is dependent on the milled depth, the milling is referred to as 2D patterning if the sputtered depth is <100 nm, and 3D micromachining if the sputtered depth is >100 nm.

FIB 2D Patterning

FIB 2D patterning is used to pattern a diverse range of materials into dots, lines, and arrays. The 2D pattern densities

achieved by FIB milling and electron beam lithography are comparable. Both techniques can routinely prepare arrays of circles or squares with 40 nm feature sizes and spacing. For smaller feature sizes and spacing, the tails of the ion beam profile may sputter away the material between the elements, and the metal lift-off step becomes difficult in electron beam lithography.

There are many examples in the literature of FIB rapid prototyping that could also have been fabricated using electron beam lithography. For instance, Allwood et al.[10] used 2D patterning to mill out 100-nm-wide lines from NiFe thin films (6 nm thick) to produce ferromagnetic inverter gates and a shift register. In another study, Toperov et al.[11] patterned 30-nm-thick NiFe thin films that were sputter-deposited onto Si_3N_4 membranes (for electron holography) into sub-500-nm arrays (i.e., a pattern of holes) to study domain pinning and magnetization reversal. FIB patterning also reduced the required handling of the membranes. Such membranes are very fragile and can be easily broken during spinning and baking of the resist and the metal lift-off step required for electron beam lithography. Enkrich et al.[12] milled split ring oscillators (as near-field metamaterials) with 100 nm feature sizes across field sizes of 320 μm^2. It reportedly took less than 30 minutes to FIB-mill each pattern, whereas it would have taken several days using electron beam lithography to optimize the exposure dose for their different patterns. A further advantage of FIB milling is that it is a maskless, direct-write process and has a large field depth, which enables it to pattern irregular and curved surfaces that are difficult to spin-coat with resists. Lugstein et al.[13] used these capabilities to fabricate organic light-emitting devices on atomic force microscope (AFM) heads for scanning near-field microscopy. Injection regions in the organic layers (deposited using a solvent-free process) were defined by FIB milling through the encapsulating insulator. Similarly, An et al.[14] milled through evaporated Cr/Au and encapsulating nitride layers to expose an electrode around an AFM tip to enable both topography and electrochemical mapping.

Micromachining 3D Structures

Conventional processing such as UV lithography and deep reactive ion etching or wet etching can be used to produce 3D structures; as the etching is parallel, these 3D structures are all to the same depth. However, with FIB milling, the dose can be varied pixel to pixel, which enables the milled depths to be varied over a pattern and structures with curved or sloping sidewalls to be prepared

One of the first 3D micromachining applications involved removing the material at the sides of AFM tips to enable measurement of high-aspect-ratio structures.[15] Typically, such milling is performed using a series of annular rings with decreasing diameters. Magnetic force scanning probes have also been machined to give small stray fields and well-defined magnetization directions. This involved sharpening sputter-coated tips[16] or shaping particles attached at the ends of the tips.[17] Figure 1 shows a magnetic CoSm particle attached to a cantilever before and after shaping.[18] For such modified tips, coercive fields of up to 2.2 T were obtained, which is close to the bulk value of CoSm.

As the dimensions of devices and structures continue to shrink, understanding their mechanical properties at the micro and nano length scales is becoming increasingly important. FIB 3D micromachining is facilitating this understanding and has been used to fabricate cantilevers,[19,20] bridges,[21] and pillars[22] and to modify nanoindenter heads.[23] Figure 2 shows an FIB-micromachined 1-μm-diameter Si pillar before and after compression with a flat punch in a nanoindenter, which was used to investigate the mechanical properties of silicon at submicron length scales. Uniaxial compression tests on single-crystal metal pillars with diameters ranging from 180 nm to 50 μm have also been performed.[22,24] The deformation occurred by localized shear on the slip system. The compressive yield stress scaled roughly as the inverse square root of the column diameter. The apparent strain hardening also increased with decreasing diameter, and stresses as large as 1 GPa were reached.

The fabrication of pillars with such high aspect ratios from a variety of materials again illustrates the advantages of FIB milling, as their manufacture would be very difficult using either wet or dry etching. The site-specific FIB micromachining capability was also used to prepare cantilevers from grains, with specific orientations determined by electron backscatter diffraction (EBSD).[25]

The nanoindentation work of Cross et al.[26] combines several of the advantages of using FIBs. Gratings and coupons were milled into 1-mm-diameter silicon balls that were imprinted using a nanoindenter to study the mechanics of nanoimprint lithography. Figure 3a shows a low-magnification secondary electron (SE) image of a Si ball in which a coupon has been FIB-milled at its center, and Figure 3b shows a high-magnification image of the coupon in which a grating has been milled.

Another FIB-based mechanical characterization technique,[27] used to measure residual strain, is based on the engineering hole method. In this method, holes with millimeter or larger dimensions are drilled into the material; image correlation is used to measure the relaxation of the material around the hole, and from this, the residual strain can be calculated. FIBs enable submicron-wide slots to be milled and this makes the analysis of local properties possible, for example across grain boundaries or within thin films (see, e.g., Reference 28).

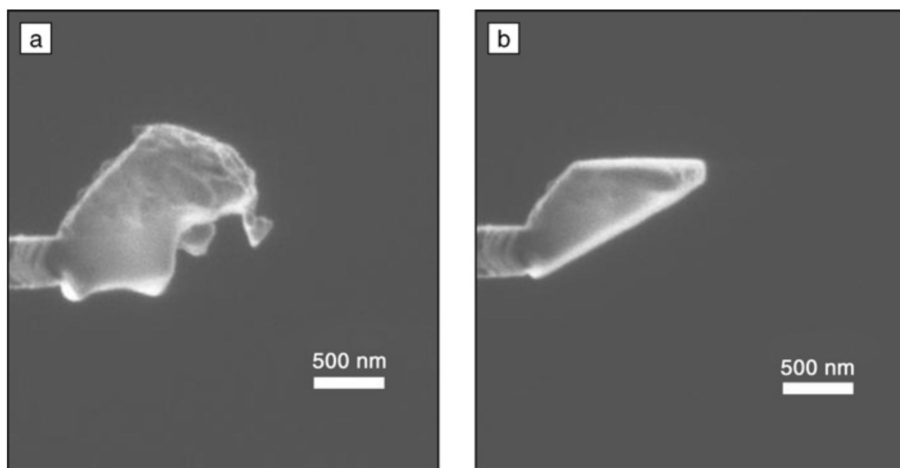

Figure 1. Shaping of a magnetic CoSm particle as an optimized magnetic force microscope tip: (a) before and (b) after focused ion beam (FIB) shaping.

Micromachining 3D Structures with Complicated Shapes

Milling 2D patterns with 100 nm feature sizes and 3D micromachining circles and

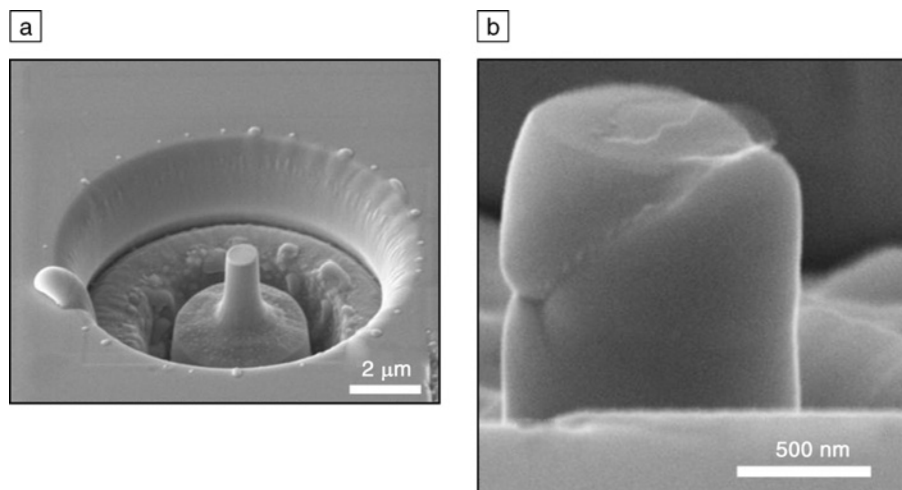

Figure 2. FIB-fabricated GaAs pillar (a) before and (b) after compression. (Figure 2b courtesy of H. Michler, EMPA Thun.)

squares (in which case, aspects such as the sidewall profile are not critical) are relatively straightforward. Even for complex 2D patterns, the effects of the ion beam profile can be corrected using a trial-and-error approach in which the dose is manually varied over the pattern. However, milling 3D structures and devices such as Fresnel lenses, whose performance is dependent on their shape, requires complicated milling strategies to achieve good fidelity between the milled and intended structure.

To improve the pattern fidelity, methods have involved changing the rastering pattern and the pixel dwell times. Nellen et al.[29] found that for photonic structures consisting of holes, different shapes were obtained depending on whether the series of concentric circles was milled with increasing or decreasing radius *r* and that the holes with the most vertical sidewalls were obtained if the dwell time was proportional to $r^{1.5}$.

More complicated approaches have accounted for the ion beam profile and the dependence of the sputter yield on the incident angle.[30,31] For structures with moderate aspect ratios, this strategy improves the fidelity, and for structures such as hemispheres and sinusoidal curves, the fidelity can be within 5%.[32] Figure 4 compares the simulated and experimental cross sections of a Fresnel lens milled in Si and shows good agreement.[30] Other strategies have also included effects such as self-focusing and redeposition.[33] These complicated strategies require knowledge of the sputter yield dependency on the incident angle, penetration depth, sticking coefficients, and backscatter angular distribution of primary ions as well as the angular distribution of the milled atoms.[34] This information can be obtained experimentally or estimated from Monte Carlo or molecular dynamics simulations. Several programs exist for this (often developed by research groups and freely available), such as SRIM[35] and GEANT.[36]

Other factors that hinder precise 3D micromachining include sputter yield changes with dose and the evolution of ripples and surface topography during milling.[37,38] For example, if a material has grains with different orientations, these may sputter at different rates, which can result in topography at the base of the FIB cut. This topography can be reduced by either changing the raster direction or milling selected areas based on the ion channeling contrast.

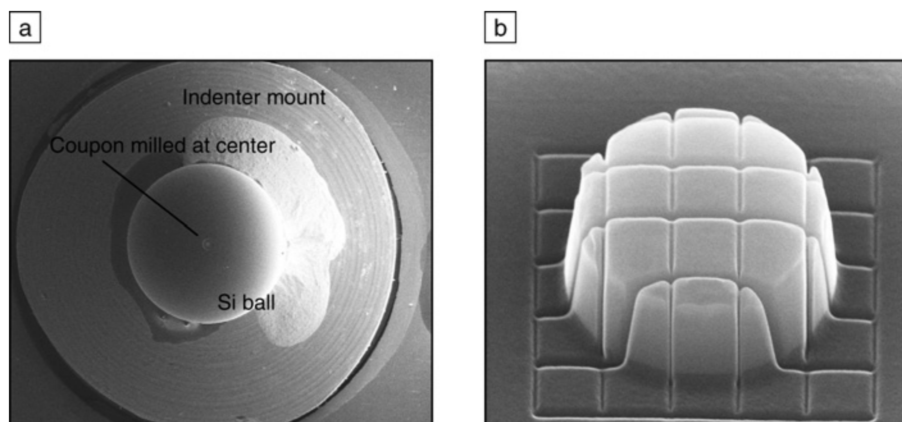

Figure 3. Secondary electron images showing (a) FIB-milled 1-mm-diameter Si ball and (b) grating FIB-milled into a coupon for use in a nanoindenter for nanoimprint lithography.

FIB Nanofabrication

In the micromachining examples previously given, the feature sizes have been 100 nm or larger. Next, FIB-based methods used to produce sub-5-nm feature sizes (sizes difficult to produce using standard fabrication processes) are discussed because of their importance in nanoengineering and nanocharacterization (e.g., contacting to nanoparticles).

Two methods involve milling through thin membranes (30–200 nm). In one, a hole, which may be hundreds of nanometers in diameter, is milled through the membrane, and either electron or ion beam SiO_2–assisted deposition is used to fill the hole and reduce its diameter. This method was used to reduce the diameter of the hole in scanning near-field optical microscope (SNOM) tips[39] that defines the diameter of the emitted beam, and to make ballistic nanocontacts by sputter-depositing Ni onto both sides of the membranes.[40] The resulting SiO_2 ring has also been used to attach DNA around the pores for biosensing.[41]

The second membrane-based method used to make sub-5-nm-diameter nanopores involves milling through the membranes and using the redeposition to produce a cone-shaped hole. If the hole diameter and milling time/dose are chosen correctly (which is a function of the membrane thickness), the apex of the cone will just cut through the rear side of the membrane.[42] Generally, Si_3N_4 membranes are used, but because charging can be an issue, SiC membranes[43] have also been used. The SiC membranes were coated with a metallic thin film to compensate for the intrinsic stress within the membranes.

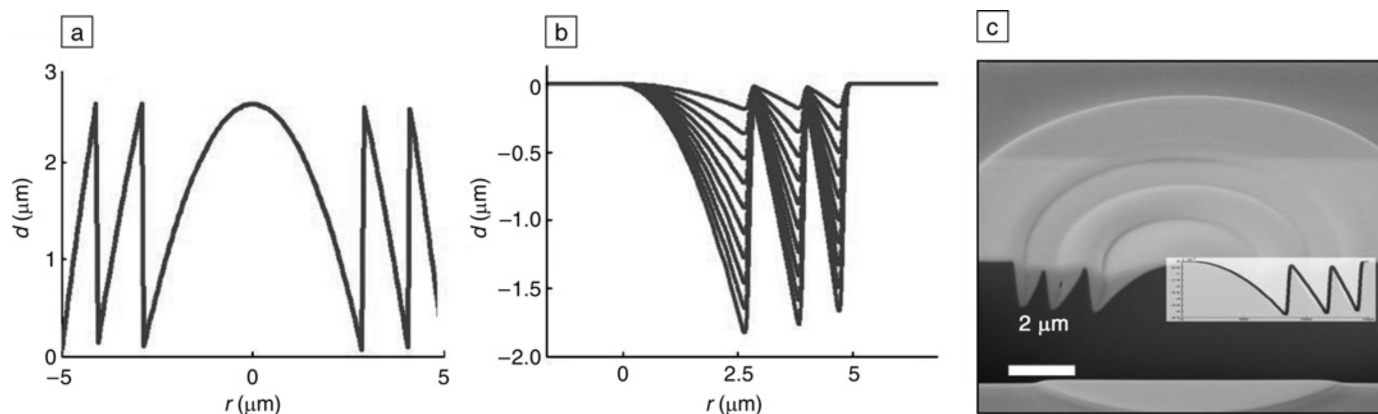

Figure 4. (a) Geometry of a Fresnel structure (*d* is depth and *r* is radius). (b) Milling simulation of a Fresnel structure. Each line corresponds to 90 passes. (c) Cross section of a milled Fresnel microlens on Si, compared with simulation (inset).

The tapering of an FIB cut as the milling depth increases was also used to make sub-5-nm planar nanogaps. Nagase et al.[44] milled a line across 30-nm-thick UV patterned gold tracks on SiO_2 and, to stop the FIB milling just as it cut through the gold track, *in situ* transport measurements were used during the milling.

Two- and three-dimensional sputtering is a physical process that may alter material properties and may adversely affect the device operation and performance. (As will be discussed later, effects such as interface mixing and implantation damage can also be deliberately used for device modification and patterning). Because the emphasis here is on FIB micro- and nanoengineering, these detrimental secondary effects are not discussed in detail. However, detrimental material changes that may occur include phase or crystallography changes, crystalline material amorphization,[45] gallium precipitation in the form of spheres/droplets that can be up to a few 100 nm in diameter,[46] interface diffusion,[47] and preferential sputtering of compound materials leading to nanodroplets.[48] See also the article by Mayer et al. in this issue for a discussion of potential sample damage from FIB.

Ion Beam Lithography

One limitation of FIB milling is that it can be time-consuming to pattern large areas. The required processing time can be reduced by using wet or dry etching to transfer an FIB-sputtered or implanted area (or the surrounding unexposed area) to the material beneath (i.e., ion beam lithography). Such two-step processes also retain the nanopatterning capabilities of the FIB and may reduce or prevent ion damage to the material underneath. For pattern transfer by dry etching, ion beam energies of less than 1 keV may be employed.

The reported line widths are generally 40–50 nm, but 15-nm-wide lines were reported using AlF_3,[49] and 6–8-nm-diameter holes were reported using poly(methyl methacrylate) (PMMA),[50] which are comparable to those obtained by electron beam lithography. The line width will depend on factors such as the mechanism for changing the etch resistance of the material (e.g., breaking C bonds via secondary electrons or vacancy generation through ion damage), beam scattering, and material sensitivity. Although the line widths obtained by ion beam exposure are as good as those by electron beam exposure, there are advantages to using the former. For organic resists, such as PMMA, the proximity effects are less, and inorganic resists such as Ti, SiN, and Si can be used.

FIB lithography was employed to make templates with graded heights for nanoimprint lithography using spin-on glass[51] and 30-nm-thick Si freestanding cantilevers and bridges.[52] Figure 5 shows 80-nm-wide lines developed in a diazonaphthoquinone novolak resist system[53] exposed with a Ga dose of 10^{12} Ga cm^{-2} and transferred by O_2 reactive ion etching. The Ga_2O_3 formed at the surface of the exposed resist acts as the etch stop, which enables thick resists to be patterned. Wet etching and FIB milling were combined to create ordered alumina nanochannels.[54] Seed holes, 3 nm in depth, matched to the lattice constant of the naturally forming array (which is dependent on the anodizing conditions) were milled into aluminum to produce an array of hcp nanochannels on anodizing.

Paralleling subtractive patterning and additive processes were also used to grow dots and wires, again exploiting the small FIB probe size. The achievable pattern densities depend on factors such as the aspect ratio of the nanostructures (generally as they grow upward, they grow outward), heat treatments (causing diffusion of induced defects and changes in surface morphology), and the interaction mechanism of the material being grown with the implanted/modified area.

Additive growth was used to organize nanometer gold clusters[55] (2.8 nm in diameter and produced by a laser vaporization technique) on FIB-patterned, highly oriented, pyrolitic graphite and to grow Co dots by electrodeposition into FIB holes cut through SiO_2.[56] Vandervelde et al.[57] FIB-implanted Si(001) with low doses (10^{14} Ga cm^{-2}) to control the nucleation of expitaxial Ge nanostructures. The localization of the quantum dot nucleation to the implanted area was attributed to surface topography. A transient surface morphology that comprised a nanoscale annular depression that sharpened to a single point and then disappeared occurred during the recrystallization anneal. Sun et al. investigated the effect of dose and substrate orientation on the growth of InP lines on (001) GaAs substrates by hydride vapor-phase epitaxy. Lines were implanted at 15° intervals, and for line doses of 2×10^{10} Ga cm^{-1} and above, continuous InP wires grew but with widths dependent on the crystallographic directions.[58] InI_3 dots and wires were also fabricated by exposing FIB-irradiated areas on (100) InP substrates to iodine.[59] Figure 6 shows a 40 nm island and nanowires grown at a substrate temperature of 200°C. Surface topography and native oxide effects were identified as factors determining the growth localization to the implanted areas.

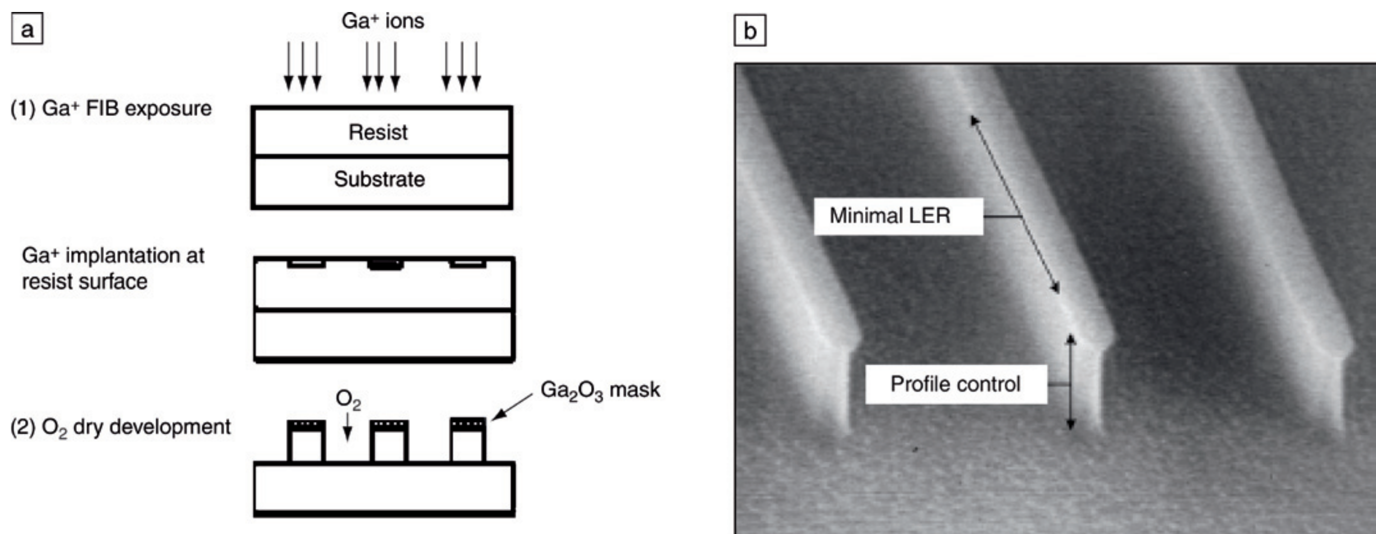

Figure 5. (a) Process steps and (b) secondary electron image of lines patterned using ion beam lithography and dry etching.

FIB milling of some materials can also result in the formation of nanodots, nanoneedles, and nanowires without an additive or subtractive step. This self-organization was attributed to preferential milling, alloying, and defect/dislocation formation and resulted in 20-nm-wide Sb and GaSb wires and In nanoparticles.[60–62]

Ion Implantation

This section discusses FIB implantation for patterning and controlled modification of material properties. As with FIB milling, one of the advantages of FIB implantation is that this is a maskless direct process capable of patterning line widths as narrow as 10 nm. Furthermore, the dose can be varied pixel by pixel, and this makes possible the modification of devices and materials at length scales that are difficult to achieve using conventional processing techniques. Ion implantation and the associated secondary effects, such as interface mixing, have been used to fabricate quantum-effect structures such as quantum wires,[63] single-electron transistors,[64] in-plane gated structures,[65] and diodes.[66] Shen et al.[67] fabricated laterally graded and asymmetric junctions to modify the threshold voltages and to reduce hot-electron effects in submicron metal oxide semiconductor field-effect transistor devices. Ion implantation–induced mixing was used in semiconductor heterojunctions to define distributed feedback lasers[68] and channel waveguides in superlattices.[69] FIBs were also incorporated into molecular beam epitaxy systems for the fabrication of modulation-doped layers and buried nanostructures.[70,71]

For magnetic materials, FIB implantation alters the coercivity and anisotropy direction of NiFe thin films,[72] the bias field strength and direction in exchange-biased layers, and the moment orientation in Co/Pt multilayers.[73] FIB patterning was used to create arrays of nanometer-sized dots and lines to investigate interdot coupling, reversal dynamics, and dipolar interactions of submicron magnetic elements.[74–76] Vieu et al.[77] patterned lines into Pt/Co/Pt trilayers: depending on the line dose, the preferred perpendicular anisotropy remained (albeit at a reduced value) or was changed to being paramagnetic. This was used to realize arrays experiencing either exchange or dipolar coupling. McGrouther and Chapman[78] implanted CoFe layers to create alternating 3-μm-long and 1-μm-long, 100-nm-wide wires. They observed, using Lorentz transmission electron microscopy imaging, that the longer wires reversed at a lower field, resulting in the formation of an ordered array of domains.

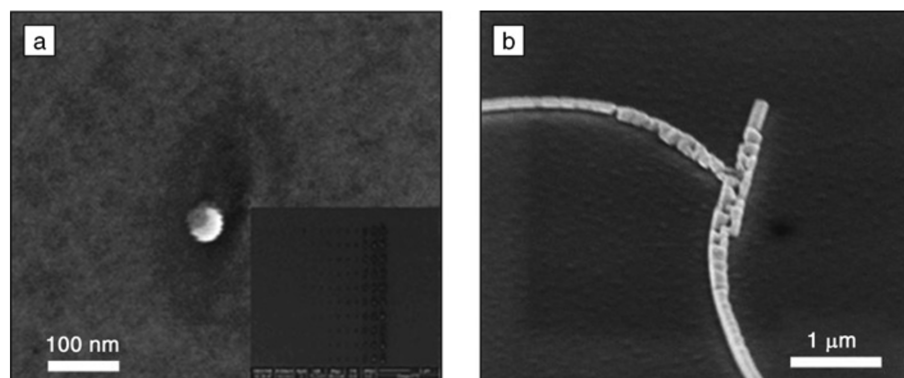

Figure 6. (a) dots and (b) InI_3 wires grown on an FIB-irradiated (100) InP substrate.

Other Fabrication Techniques

This section highlights some of the other micro- and nanocapabilities of the FIB systems that often bridge across the methods described in the three previous sections. Again, the examples given illustrate the diversity of use of these instruments.

In situ micromanipulation for lifting out TEM slices or wedges is discussed in the article by Mayer et al. in this issue of *MRS Bulletin*. *In situ* micromanipulation has also been used to lift up and place nanowires and nanotubes onto pre-patterned electrodes[79] and at fixed angles onto AFM tips.[80] Such micromanipulation is also performed within SEMs, but if using an FIB system, Pt deposition can be used to fix the nanowires to the tip of needle or

substrate, and the FIB can cut them once they are positioned. Another method used to orient multiwall carbon nanotubes attached to scanning probe tips involves exposing them to the ion beam.[81] Although the mechanism for the bending is unclear, it was used to orient nanotubes at 45° relative to the scanning probe tip.

The fundamentals of electron and ion beam–assisted deposition are discussed in the article by MoberlyChan et al. in this issue. Thus, only two examples, illustrating the nanofabrication potential of beam-assisted deposition, are given here. However, one should note that, similar to FIB sputtering, this fabrication process is maskless; metals or insulators can be deposited to within 50 nm of a particular feature of interest and high-aspect-ratio structures may be prepared.

Electron beam–assisted deposition has used to deposit 60-nm-wide Pt nanopillars to act as both a hard mask and a self-aligned top contact for patterning spin valves[82] by dry etching. Such structures can be made using electron beam lithography but require up to eight processing steps, making the fabrication considerably more difficult, and this results in a lower success yield. Pt ion beam–assisted deposition, over holes in nitride membranes, has been used to reproducibly fabricate 2-nm-wide nanogaps, gap sizes that would be very difficult to prepare using any other lithography technique. (The tunneling current was measured to control the end point.) Bridging over a hole by sequentially offsetting the Pt deposition area prevents the Pt "halo" (due to the secondary electrons generated from backscattered electrons) from shorting around the nanogap.[83]

All of the FIB nanoengineering examples given in this article used a Ga ion beam. However, alloy sources, coupled with mass separators to select a particular ion species, may also be used. This offers many other avenues for device fabrication and modification. For example, Bischoff et al.[84] used $Co_{36}Nd_{64}$ alloy sources and implanted Co into Si(111) wafers to produce 10 nm $CoSi_2$ wires on annealing. Reuter et al.[85] implanted Be and Si to create *p*- and *n*-type GaAs and studied the effect of this on self-assembled growth of InAs dots.

Future Outlook

The smallest spot size of an FIB system is approximately 5 nm. Smaller spot sizes, while maintaining or increasing the current densities, would further enhance the system's nanofabrication capabilities, especially if the improvements also occur at lower energy. Moderate improvements might be possible with current liquid-metal ion source technology; however, other source types may be required, such as magneto-optical trap ion sources.[86] Different sources and column designs will possibly be required for different applications, and system differentiation may occur; systems specialized for nanofabrication (e.g., with alloy sources and small probe sizes) and for sample preparation for electron microscopy (e.g., with larger spot sizes and current densities) may be developed.

Currently, the tendency is to automate the systems as much as possible. However, another type of specialized system could be one that gives users greater control of the hardware and software. This would then provide research institutions with greater freedom in incorporating them with other fabrication tools, such as low-energy sputter guns.

In addition to systems with smaller spot sizes, another development would be the availability of precursor gases for depositing other pure metals such as Co and Au. This would then facilitate the rapid fabrication of, for example, spintronic devices. Currently, the commercially available precursor gases are limited (typically to W and Pt), and the deposited metals contain a large amount of carbon.

Other system developments could occur via the software. Algorithms could be incorporated into the patterning scripts to correctly mill 2D patterns and 3D shapes by taking into account aspects such as the beam profile. This would parallel proximity-correction software currently available in electron beam lithography.

This article has illustrated the nano- and microfabrication capabilities of FIB and dual-platform systems. While these techniques offer many advantages relative to conventional processing methods, among which are the ability to pattern onto irregular surfaces, FIB and dual-platform systems should still be considered as complementary tools to conventional processing. As the capabilities of the current systems—for example, reduction of the low-energy spot sizes—are further developed, it is expected that their impact within the fields of micro- and nanoengineering and nanoscience will grow.

References

1. M.T. Abramo, L.L. Hahn, *Microelectron. Reliability* **11**, 1775 (1996).
2. G. Pan et al., *J. Magn. Magn. Mater*. **202**, 583 (1999).
3. F. Lacour et al., *Opt. Lett*. **27** (8), 1421 (2005).
4. L. Kumarir, S.V. Subramanyam, *Bull. Mater. Sci*. **27** (3), 289 (2004).
5. S.N. Sharma, S.M. Shivaprasad, S. Kohli, R. Rastogi, *Pure Appl. Chem*. **74** (9), 1739 (2002).
6. F. Schiappelli et al., *Microelectron. Eng*. **73**, 397 (2004).
7. C.W. Leung, C. Bell, G. Burnel, M.G. Blamire, *Phys. Rev. B* **72**, 212409 (2005).
8. H. Lohmeyer et al., *J. Eur. Phys. B* **48**, 291 (2005).
9. S.-J. Kim et al., *Physica C* **412**, 1401 (2004).
10. D.A. Allwood et al., *Science* **296**, 2003 (2002).
11. A. Yu Toporov, R.M. Langford, A.K. Petford-Long, *Appl. Phys. Lett*. **77**, 3065 (2000).
12. C. Enkrich et al., *Adv. Mater*. **17**, 2547 (2005).
13. A. Lugstein et al., *Appl. Phys. Lett*. **81** (2), 349 (2002).
14. K.H. An et al., *Appl. Phys. Lett*. **89**, 111117 (2006).
15. H. Ximen, P.E. Russell, *Ultramicroscopy* **42**, 1526 (1996).
16. Z. Liu, Y. Dan, Q. Jinjun, Y. Wu, *J. Appl. Phys*. **91** (10), 918843 (2002).
17. L. Gao et al., *IEEE Trans. Magn*. **40** (4), 2194 (2004).
18. P.N. Nellen, V. Callegari, U. Sennhauser, *Chimia* **60** (11), 735 (2006).
19. S. Reyntjens, R. Puers, *J. Micromech. Microeng*. **10**, 181 (2000).
20. C. Motz, T. Schoberl, R. Pippan, *Acta Mater*. **53**, (2005) p. 4269.
21. J. McCarthy, Z. Pei, M. Becker, D. Atteridge, *Thin Solid Films* **358**, 146 (2000).
22. M.D. Uchic, D.M. Dimiduk, W.D. Nix, *Science* **305**, 986 (2004).
23. P. Trtik, C.M. Reeves, P.J.M. Bartos, *Mater. Struct*. **33**, 189 (2000).
24. C.A. Volkert, E.T. Lilleodden, *Philos. Mag*. **86** (33), 5567 (2006).
25. D.I. Maio, S.G. Roberts, *J. Mater. Res*. **20** (2), 299 (2005).
26. G. Cross, B. O'Conner, R.M. Langford, J. Pethica, *Mater Res. Soc. Symp. Proc*. **841**, R1.6.1 (Warrendale, PA, 2005).
27. K.J. Kang, S. Darzens, G.S. Choi, *J. Eng. Mater. Technol*. **126**, 457 (2004).
28. P. Jud, P.M. Nellen, U. Sennhauser, *Adv. Eng. Mater.* **7** (5), 384 (May 2005).
29. P.M. Nellen, V. Callegari, R. Brönnimann, *Microelectron. Eng*. **83**, 1805 (2006).
30. D.P. Adams, M.J. Vasile, T.M. Mayer, *J. Vac. Sci. Technol. B* **24** (4), 1766 (2006).
31. M.J. Vasile, W. Zhang, *J. Vac. Sci. Technol. B* **17** (6), 3085 (1998).
32. D.P. Adams, T.M. Mayer, M.J. Vasile, K. Archuelta, *Appl. Surf. Sci*. **252**, 2432 (2006).
33. E. Platzgummer et al., *Microelectron. Eng*. **83**, 936 (2006).
34. P.M. Nellen et al., in *Mater Res. Soc. Symp. Proc*. **983E** (2006) paper no. 0960-N10-03-LL06-03.
35. J.F. Ziegler, J.P. Biersack, *The Stopping and Range of Ions in Solids* (Pergamon Press, New York, 1985).
36. M.H. Mendenhall, R.A. Weller, *Nucl. Instrum. Methods Phys. Res*. **227**, 420 (2005).
37. S. Rusponi, G. Costantini, F. Buatier de Mongeot, U. Valbusa, *Appl. Phys. Lett*. **75** (21), 3318 (1999).
38. N.P. Hung, Y.Q. Fu, M.Y. Ali, *J. Mater. Process. Technol*. **5763**, 1 (2002).

39. A.M. Minor, V.R. Radmilovic, E.A. Stach, T. Schenkel, *Microsc. Microanal*. **10**, 1118 (2004).
40. R.M. Langford, T.-X. Wang, *J. Nanosci. Nanotechnol*. **6** (9), 343 (2006).
41. J. Nilsson, J.R.I. Lee, T.V. Ratto, S.E. Letant, *Adv. Mater*. **18**, 427 (2006).
42. H.-X. Wei, R.M. Langford, X.-F. Han, J.M.D. Coey, *Appl. Phys. Lett*., **99** (8), 501 (2006).
43. A.-L. Biance et al., *Microelectron. Eng*. **83**, 1474 (2006).
44. T. Nagase, K. Gamo, T. Kubota, S. Mashiko, *Micro. Elec*. **78**, 253 (2005).
45. V. Hodzic, J. Orloff, C.C. Davis, *J. Lightwave Technology* **6** (22), 209 (2004).
46. J. Reiner, P. Nellen, U. Sennhauser, *Microelectron. Reliability* **44** (9), 1583 (2004).
47. T.J. Colla, H.M. Urbassek, *Phys. Rev. B* **6310** (10), 2002 (2001).
48. U. Müller, U. Sennhauser, F. Hernández-Ramírez, *Appl. Surf. Sci*. (2006) submitted.
49. J. Gierak, A. Septier, C. Vieu, *Nucl. Instrum. Methods Phys. Res. Sect. B* **127**, 893 (1997).
50. R.L. Kubena et al., *J. Vac. Sci. Technol. B* **9**, 3079 (1991).
51. J. Taniguchi, K. Koga, Y. Koga, I. Miyamoto, *Microelectron. Eng*. **83**, 940 (2006).
52. R.M. Langford, A.K. Petford-Long, M. Rommeswinkle, S. Egelkamp, *Mater. Sci. Technol*. **18**, 743 (2002).
53. S.F. Gilmartin et al., *Microelectron. Eng*. **83**, 823 (2006).
54. C.Y. Liu, A. Datta, Y.L. Wang, *Appl. Phys. Lett*. **78** (1), 120 (2001).
55. A. Perez et al., *New J. Phys*. **4**, 76.1 (2002).
56. M.V. Rastei et al., *J. Magn. Magn. Mater*. **286**, 10 (2005).
57. T.E. Vandervelde et al., *J. Vac. Sci. Technol. A*, **24** (2), 375 (2006).
58. Y.T. Sun et al., *Appl. Phys. Lett*. **79** (12), 1185 (2001).
59. V. Callegari, P.M. Nellen, *Phys. Status Solidi A* (2006) submitted.
60. Y.Z. Huang, *Appl. Phys. Lett*. **88**, 103104 (2004).
61. A. Lugstein, J. Bernardi, C. Tomastok, E. Bertagnolli, *Appl. Phys. Lett*. **88**, 163114 (2006).
62. N. Nitta, M. Taniwaki, *Nucl. Instrum. Methods Phys. Res. Sect. B* **24**, 234 (2004).
63. A.D. Wieck, K. Ploog, *Appl. Phys. Lett*., **56**, 928 (1990).
64. T.W. Kim et al., *Solid State Commun*. **115**, 77 (2000).
65. W.F. Tseng, D.H. Monk, *Mater. Lett*. **40**, 235 (1999).
66. S. Nakata, *Phys. Rev. B* **46**, 13326 (1992).
67. C. Shen et al., *IEEE Trans. Electron Dev.* **45** (2), 453 (1998).
68. A.J. Steckl et al., *J. Vac. Sci. Technol. B* **13** (6), 2570 (1995).
69. D.H. Naghski, J.T. Boyd, H.E. Jackson, A.J. Steckl, *Opt. Commun.* **150** (6), 97 (1998).
70. T. Goto et al. *Appl. Sur. Sci*. **159**, 277 (2000).
71. J.H. Thompson et al., *J. Appl. Phys*. **74**, 4375 (2005).
72. S.1. Woods et al., *Appl. Phys. Lett*. **81**, 1267 (2002).
73. C. Chappert et al., *Science* **280**, 1919 (1998).
74. N. Owen, H.-Y. Yuen, A. Petford-Long, *IEEE Trans. On Magn*., **38** (5), 202 (2002).
75. J. Fassbender et al., *Phys. Status Solidi A* **189**, 439 (2001).
76. P. Warin et al., *J. Appl. Phys*. **90**, 3850 (2001).
77. C. Vieu et al., *Phys. Rev. Lett*. **81**, 5656 (1998).
78. D. McGrouther, J.N. Chapman, *Appl. Phys. Lett*. **87**, 22507 (2005).
79. R.M. Langford, T.-X. Wang, A. Heidelberg, J.G. Sheridan, *J. Vac. Sci. Technol. B* **24**, 2306 (2006).
80. A. Hall et al., *Appl. Phys. Lett*. **82**, 2506 (2003).
81. Z. Deng et al., *Appl. Phys. Lett*. **88**, 23119 (2006).
82. H.X. Wei et al., *J. Magn. Magn. Mater.* **303** (2), 208 (August 2006).
83. K. Shigeto et al., *Microelectron. Eng*. **83**, 1471 (2006).
84. L. Bischoff, B. Schmidt, Ch. Akhmadaliev, A. Mucklich, *Microelectron. Eng*. **83**, 800 (2006).
85. D. Reuter et al., *Mater. Sci. Eng*. **23**, 456 (2001).
86. J.L. Hanssen, E.A. Dakin, J.J. McClelland, *J. Vac. Sci. Technol. B* **24** (6), 2907 (2006).

www.mrs.org/fall2007
CALL FOR PAPERS
ABSTRACT DEADLINE: JUNE 20, 2007
REMINDER: In fairness to all potential authors, late abstracts will not be accepted.

Meeting Chairs:

Duane Dimos
Sandia National Laboratories
Tel 505-844-6385
Fax 505-844-1583
dbdimos@sandia.gov

Mary Galvin
Air Products and Chemicals, Inc.
Tel 610-481-1524
Fax 610-481-7719
galvinme@airproducts.com

David Mooney
Harvard University
Tel 617-384-9624
Fax 617-495-9837
mooneyd@deas.harvard.edu

Konrad Samwer
Universitaet Goettingen
I. Physikalisches Institut
Tel 49-551-397601
Fax 49-551-3912229
ksamwer@gwdg.de

For additional meeting information, visit the MRS Web site at
www.mrs.org/meetings/

Member Services
Materials Research Society
506 Keystone Drive
Warrendale, PA 15086-7573
Tel 724-779-3003 • Fax 724-779-8313
E-mail: info@mrs.org • www.mrs.org

SYMPOSIA

CHARACTERIZATION APPROACHES
A: Combinatorial Methods for High-Throughput Materials Science
B: Nanoscale Phenomena in Functional Materials by Scanning Probe Microscopy
C: Quantitative Electron Microscopy for Materials Science
D: Materials in Transition–Insights from Synchrotron and Neutron Sources
E: Theory, Modeling, and Numerical Simulation of Multiphysics Materials Behavior

ELECTRONICS, OPTICS, AND MAGNETICS
F: Interfaces in Organic and Molecular Electronics III
G: Large-Area Processing and Patterning for Active Optical and Electronic Devices
H: Nanostructured Solar Cells
I.: Nanoscale Magnetic Materials and Applications
J.: Spin-Injection and Spin-Transfer Devices
K: Ferroelectrics, Multiferroics, and Magnetoelectrics
L: Zinc Oxide and Related Materials
M: Materials and Hyperintegration Challenges in Next-Generation Interconnect Technology
N: Materials, Integration, and Technology for Monolithic Instruments II
O: Nuclear Radiation Detection Materials
P: Diamond Electronics–Fundamentals to Applications II
Q: Nitrides and Related Bulk Materials

ENERGY AND ENVIRONMENT
R: Life Cycle Analysis for New Energy Conversion and Storage Systems
S: Materials and Technology for Hydrogen Storage
T: Materials Innovations for Next-Generation Nuclear Energy
U: Thermoelectric Power Generation
V: Materials Science of Water Purification

GENERAL
W: Forum on Materials Science and Engineering Education for 2020
X: Frontiers of Materials Research
Y: Materials Issues in Art and Archaeology VIII

ENGINEERED MATERIALS
Z: Bulk Metallic Glasses
AA: Fundamentals of Nanoindentation and Nanotribology IV
BB: Magnetic Shape Memory Alloys
CC: Materials for New Security and Defense Applications
DD: Microelectromechanical Systems–Materials and Devices
EE: Phonon Engineering–Theory and Applications
FF: Synthesis and Surface Engineering of Three-Dimensional Nanostructures

NANOSYSTEMS
GG: Excitons and Plasmon Resonances in Nanostructures
HH: Nanophase and Nanocomposite Materials V
II: Nanotubes and Related Nanostructures
JJ: Nanowires–Novel Assembly Concepts and Device Integration
KK: Nanoscale Pattern Formation

SOFT MATTER AND BIOSCIENCE
LL: Bioinspired Polymer Gels and Networks
MM: Biomolecular and Biologically Inspired Interfaces and Assemblies
NN: Protein and Peptide Engineering for Therapeutic and Functional Materials
OO: Solids at the Biological Interface
PP: Quantum-Dot and Nanoparticle Bioconjugates–Tools for Sensing and Biomedical Imaging
QQ: Electroactive and Conductive Polymers and Carbon Nanotubes for Biomedical Applications

MEETING ACTIVITIES

Symposium Tutorial Program
Available only to meeting registrants, the symposium tutorials will concentrate on new, rapidly breaking areas of research.

Exhibit
A major exhibit encompassing the full spectrum of equipment, instrumentation, products, software, publications, and services is scheduled for November 27–29 in the Hynes Convention Center. Convenient to the technical session rooms and scheduled to complement the program, the MRS Fall Exhibit offers everything you need all under one roof.

Publications Desk
A full display of over 935 books will be available at the MRS Publications Desk. Symposium Proceedings from both the 2006 MRS Spring and Fall Meetings will be featured.

Student Opportunities
Graduate students planning to attend the 2007 MRS Fall Meeting are encouraged to apply for a Symposium Assistant position and/or a Graduate Student Award. Applications will be accessible on the MRS Web site by May 15.

Career Center
A Career Center for MRS members and meeting attendees will be open Tuesday through Thursday.